

STATISTICS OF TLP TENDON TENSION BEHAVIOUR DURING HURRICANE LILI

Alberto Morandi
American Global Maritime
11767 Katy Freeway Suite 660
Houston, Texas, 77079

Alberto.morandi@globalmaritimeus.com

Diego Martinez
American Global Maritime
11767 Katy Freeway Suite 660
Houston, Texas, 77079

dmartinez@globalmaritimeus.com

Charles Smith
Minerals Management Service
Engineering and Research Branch
381 Elden Street, MS 4021
Herndon, Virginia, 20170
smithc@mms.gov

Keywords: Hurricane Lili, TLP, Tendon Performance

ABSTRACT

Hurricane Lili permitted an assessment of the global performance of several deepwater structures under a major environmental event. The US Minerals Management Service (MMS) commissioned American Global Maritime Inc. (AGMI) to collect and assess information on the performance of the deepwater production facilities that were impacted by Lili.

The Shell Brutus Tension Leg Platform (TLP) provided comprehensive measurements of winds, motions and tendon tensions during Lili. The tendon tension data recorded was analyzed in both the time and frequency domain and tendon tension statistics were comparable to the relevant design values. Other relevant comparisons included natural period and damping estimates.

Overall the design 'recipe' adopted for Brutus was sufficient to prevent exceedance of design capacities and damage to the hull structure and tendons during Hurricane Lili. The lessons learned from the analyses and recommendations for further work are also summarized in this paper.

1 INTRODUCTION

In recent years, exploration and production of hydrocarbons has been steadily moving into deep water. In the Gulf of Mexico there are currently 30 production units in over 1000 ft of water depth, with more to be added in the future. The evaluation of the performance of shallow water fixed platforms during major environmental events permitted significant improvements in their design and operation. Hurricane Lili provided a unique opportunity to perform such an assessment for deep water floating production units.

Hurricane Lili was the most intense hurricane of the 2002 season. As it moved across the Caribbean, Lili fluctuated in intensity and was a Category 1 hurricane near western Cuba on October 1st, 2002. Between Cuba and Louisiana, Lili intensified to 145 knots wind speed (Category 4 Hurricane) on October 2nd, 2002 and maintained intensity into October 3rd, 2002. It suddenly lost intensity and was a much weaker hurricane by landfall.

Lili was a Category 4 hurricane while over the north-central Gulf of Mexico and during the early hours of October 3rd, 2002 it passed through the Green Canyon and Eugene Island areas, impacting several Tension Leg Platforms (TLPs) and a spar, Figure 1 and Table 1.



Figure 1 –Floating Production Units near Lili’s Track

Table 1 – Floating Production Units near Lili’s Track

FPU	Type	Operator
Typhoon	Mono-Column TLP	ChevronTexaco
Morpeth	Mono-Column TLP	ENI Petroleum
Allegheny	Mono-Column TLP	ENI Petroleum
Jolliet	4-Column TLP	Conoco
Genesis	Spar	ChevronTexaco
Brutus	4-Column TLP	Shell
Prince	TLP	El Paso

A hindcast study¹ permitted the maximum environmental conditions such units were exposed to be estimated and the results are given in Table 2.

Table 2 – Hindcast Environmental Conditions¹

FPU	Hindcast		
	Wind* (knots)	Significant Wave Height (ft)	Current (knots)
Typhoon	71.22	37.04	2.15
Morpeth	43.17	30.11	1.98
Allegheny	50.13	33.30	1.83
Jolliet	50.30	30.97	1.53
Genesis	54.46	35.11	2.50
Brutus	59.83	36.75	1.80
Prince	46.13	32.09	2.00
Buoy 42041	64.98	37.73	-

*1/2-hour mean at 10m above sea level

It is noted that the data in Table 2 is based purely on the hindcast results. The hindcast wind fields and seastate model were well validated¹ against a fairly comprehensive set of data ranging from buoys of the National Data Buoy Center (NDBC) to aircraft reconnaissance as well as satellite meteorological

data. Based on such data, the bias in wave height and period were of the order of 0.1m and 0.5 sec respectively. One of such buoys was within 40 miles of some of the units in Table 1 and is included in Figure 1 and Table 2. No in-situ current data were available for the hindcast so it was not possible to make any direct assessment of the quality of the Lili current hindcast data.

Additional data were identified in this project for the units in Table 1 (wind measurements at Brutus and current measurements near Genesis) which were not available to the hindcast. This additional measured data compares reasonably well with the hindcast although some discrepancies were found concerning wind velocities and current velocities. The hindcast and measurements were also compared to typical design values for environmental conditions. Detailed results of such comparisons are discussed in an upcoming OTC paper².

Overall the wind velocity and wave height values given for the Brutus TLP in Table 2 were of the order of 90% of the 100-year design environmental conditions.

2 RELIABILITY OF TLP PLATFORMS

The reliability of TLPs has been extensively investigated and many publications by well known experts in the field can be found in the open literature³⁻²². The global performance of the early TLP structures (Hutton, Heidrun and Snorre) was investigated²³⁻²⁶ under operating conditions and winter storms and concluded to be within design expectations.

The knowledge gained from such work has enabled the development of rational procedures for the safe design of TLPs which are covered in industry standards such as API RP 2T²⁷. Prediction of tendon tensions is a critical part of such design procedures. Tendon strength is verified against the predicted maximum tendon tension. It is good design practice to verify that tendon tensions remain positive for the design environmental conditions. Fatigue of the tendons is also verified.

More recently, deep water production facilities in the Gulf of Mexico have experienced operational issues (prior to Lili) due to aspects such as vortex induced platform motions, the effect of gaps between the air cans and guide supports in spars under wave induced platform motions, vortex shedding effects on tendons and / or risers. These are complex issues that affect different platforms in different ways but the impact of eddy currents on TLP vortex induced vibration (VIV) was well documented²⁸ for the Allegheny TLP during the ‘Millennium’ loop current event. The whole event lasted for two months with a steady buildup of current over about a six weeks period leading to the highest estimated current of 3.4 knots. It was verified that tendon VIV caused loads and accelerations into the hull and deck which deserved more detailed investigation due to their potential impact on fatigue life.

As far as hurricanes are concerned, the Jolliet TLP was in operation during Hurricane Andrew but it was not in the direct path of that event. The data for Brutus during Lili is therefore a valuable addition to the existing knowledge of TLP performance under major environmental events.

The Brutus TLP was installed in June 2001 and is operated by Shell in Green Canyon block 158 in 2958 ft of water. Brutus is a TLP design consisting of four columns and four pontoons with a total of twelve tendons and shares much in common with its predecessor and sister vessel, the Mars TLP. The design of Brutus relied heavily on knowledge gained from the Mars design process.

Monitoring data was captured by Shell for the Brutus TLP during Lili and made available to this project. Table 3 summarizes the Brutus instrumentation system and its operational condition during Lili. It can be seen that almost all instruments were operational except for the wave probe.

Table 3: Brutus Instrumentation

	Method	Sampling Rate (Hz)	Location	Operational
Surge	DGPS	1	Quarters	Yes
Sway	DGPS	1	Quarters	Yes
Roll	Accelerometer	2	Columns	Yes
Pitch	Accelerometer	2	Columns	Yes
Heave	Accelerometer	.3	Columns	Yes
Wind	Anemometer	2	278' / 350' above keel	Yes
Wave	Probe	2	Drilling Module	No
Tendon Tension	Strain Gauge	2	Tendon top	Yes

Tendon tension data was captured for a tendon in each corner as shown in Figure 2.

The measurements and the hindcast data from Buoy 42041 showed that winds changed their mean direction as the hurricane developed its peak intensity. Over a period of 3 hours that contained the peak wind velocity, wind direction changed from approximately 80 degrees to 200 degrees. The change in wind direction was also observed in the Brutus measurements from approximately 50 degrees to approximately 240 degrees. These values refer to the direction the wind is blowing from, measured clockwise from North as shown in Figure 2.

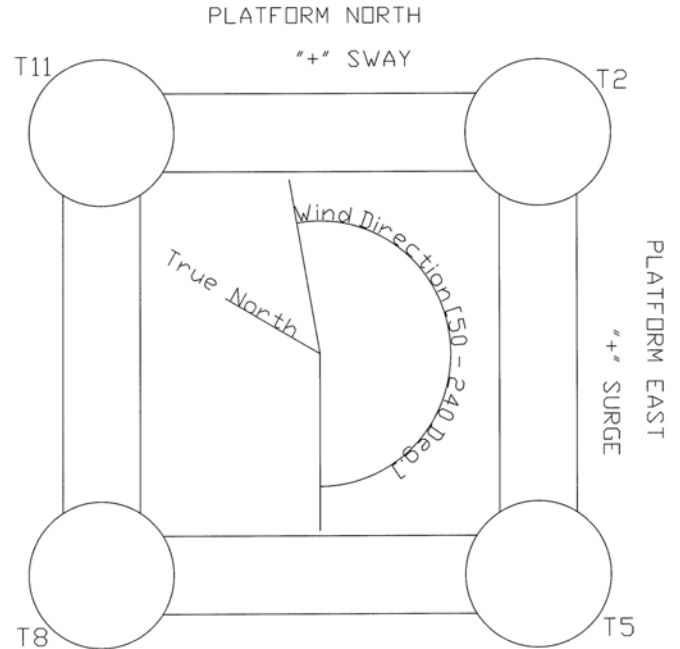


Figure 2 – Location of Instrumented Brutus TLP Tendons

3 TLP TENDON TENSIONS – DESIGN APPROACH

Standard linear models for a fully developed, wind-generated sea (no swell) assume the water surface elevation is formulated as a stationary, narrow-banded Gaussian (normally distributed) process. The peaks of this process (such as the wave heights or the wave crests), assumed as statistically uncorrelated, are then represented by a Rayleigh distribution:

$$\text{Prob}(X > x) = \exp(-2x^2) \quad (1)$$

Where x is the ratio between an individual wave height H and the significant wave height H_s .

The maximum peaks of the process (that is, the maximum waves in the seastate) can be described by a Gumbel distribution. The probability distribution for the largest individual wave normalized by the significant wave height (X_N) amongst a large number N of waves is:

$$\text{Prob}(X_N < y) = \exp\{-\exp[-(y - a_N) / b_N]\} \quad (2)$$

$a_N = 0.5 (2 \ln N)^{1/2}$ is the modal or most probable maximum value of the wave height normalized by H_s

$$b_N = a_N / (2 \ln N)$$

The same standard models and statistics discussed above for wave heights can be applied to the responses of a linear system to linear Gaussian input.

However, non-linear effects are known to cause TLPs to have a non-Gaussian quality to their response as discussed in several references³⁻²². In other words, the probability of exceeding a given level of response may exceed the values predicted by equations (1) and (2).

In order to cover these non-linear and non-Gaussian deviations, a ‘design recipe’ approach is often used in design. According to API RP 2T²⁷ the following needs to be considered:

- Pretension at mean sea level
- Tide / surge variation
- Overturning due to wind and current
- Set-down due to static and slowly varying offset
- Wave forces / wave induced motions about the mean offset
- Foundation mis-positioning
- Ringing and springing
- Tendon load sharing
- Vortex shedding
- Other design margins

The approach taken in the design of the Brutus TLP can be summarized in the equations²⁹ below:

$$T_{max} = T_{mean} + [T_{unc} + T_{mis} + \Gamma \sqrt{(\gamma^2 T_{rms}^2 + T_{rra}^2)}] \quad (3)$$

$$T_{min} = T_{mean} - [T_{unc} + T_{mis} + \Gamma \sqrt{(\gamma^2 T_{rms}^2 + T_{rra}^2)}] \quad (4)$$

T_{max} , and T_{min} are the maximum and minimum tendon tensions. T_{mean} is the mean tension due to static effects such as pretension, tide / surge variation, overturning due to static wind and current. T_{mis} covers modeling uncertainties and general design margins while T_{mis} covers foundation mispositioning. T_{rms} is the root mean square (RMS) dynamic tendon tension due to low- and wave-frequency components, calculated from a numerical model. A correction factor γ is introduced to account for deviations between numerical predictions of T_{rms} and model test results. T_{rra} accounts for resonant-frequency tension variations due to nonlinear ringing and springing excitation of the TLP in its vertical modes as well as any contribution from VIV and is estimated directly from model tests. The Γ parameter accounts for the non-Gaussian quality of the response based on tendon tension statistics derived from model test data.

The design recipe above was compared with the measurements in terms of the following:

- Time-domain analysis: Maximum and minimum values
- Time-domain analysis: Statistics of tendon tension
- Frequency domain analysis: Major response components, natural frequencies and damping

4 FREQUENCY DOMAIN RESULTS

4.1 Natural Periods

The frequency domain analysis was carried out to verify natural frequencies, energy content and damping estimates. Considering its entire duration, Hurricane Lili was clearly not a stationary process but it was assumed as stationary for periods of one hour. This stationary one-hour data was further broken down into ten-minute time series to create six independent zero-mean realizations per hour.

Power Spectral Densities (PSD) of the tendon data were then computed for these ten-minute realizations. The PSDs of these ten minutes blocks were then averaged to give a single PSD for each hour. This procedure was carried out for all tendon data to reduce the jaggedness and error of the equivalent hourly PSD computed alone. For consistency with the time domain analysis presented further in the paper, the same nine hours containing the peak hurricane data was analyzed using this averaging method.

Table 4 contains the natural frequencies for Brutus. The response at the wave peak energy (approximately 12 seconds which in good correlation with the hindcast study¹) as well as the resonance behavior may be viewed in Figure 3 which shows a typical PSD for surge. Figure 3 also shows wave loading at a frequency corresponding to waves with a length similar to the column spacing.

Table 4: Natural Periods at Relevant Load Condition

	Period (s)	Frequency (rad/sec)
Surge	118	0.05
Sway	132	0.05
Heave	3.55	1.77
Roll	3.34	1.88
Pitch	3.2	1.96

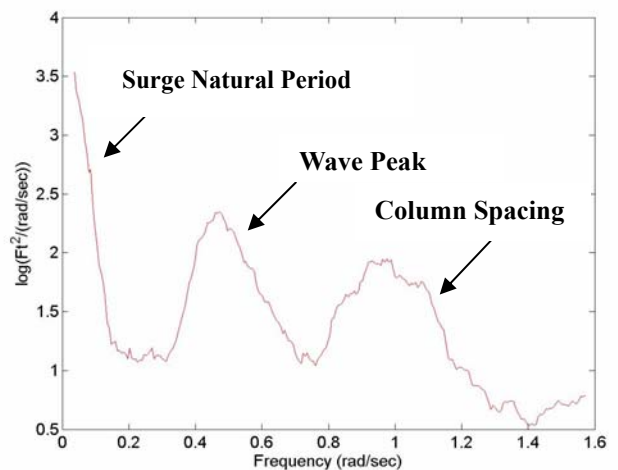


Figure 3 – Example Surge PSD

Figure 4 shows a PSD for tendon tension (tendon T2). The energy at the slow drift range (around 0.06 - 0.13 rad/sec or 50 - 100 sec) is dominant and was excluded from Figure 4 to permit a better visualization of the other components. Figure 4 also excludes the high frequency vortex shedding components which are discussed later in the paper.

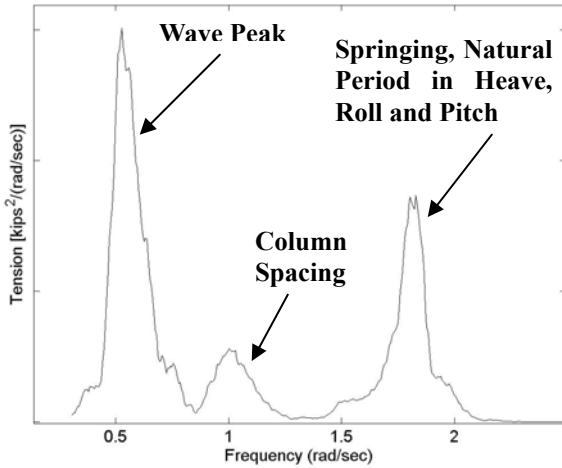


Figure 4 – PSD for Tendon Tension (T2)

4.2 Damping

Damping may significantly affect design predictions but it is not easy to quantify for a complex dynamic system such as a TLP. Damping estimates were obtained here from spectral analyses of the full-scale measured data using the half bandwidth method.

Investigations^{30,31} of the half bandwidth method as applied to offshore platform response to wave and wind loading suggest that damping estimates using the half-bandwidth method are a function of frequency resolution and typically have errors of the order of ten to twenty percent. The required frequency resolution for half bandwidth estimates for a TLP has been estimated³¹ to be a minimum of four half bandwidth points around the spectral peak. Tendon tensions were recorded at 2 Hz and for the ten-minute realizations considered here there are in excess of 100 points around the peaks which should provide sufficient resolution for damping estimates. However, it should be recognized that the underlying process was seen to be inherently non-stationary and the measured data represents purely a set of realizations of a random process. The available information concerning the environmental conditions was less than complete and therefore did not permit an independent verification of the estimated damping values.

Table 5 contains the wave frequency surge and sway damping estimates using the half-bandwidth method for each of the hurricane 9-hour segments taken from the measurements. Likewise, Table 6 contains the results for pitch and roll damping. The damping estimated for surge and sway from the measurements was in good agreement with the values used in

design which were 11.5-11.8%. The damping estimated for pitch and roll from the measurements exceeded the value used in design which was of 0.4%.

It is noted that the roll and pitch resonance in the measurements may contain heave resonance as well, since their respective natural frequencies are nearly identical and difficult to filter out. This feature could have an influence in the larger damping values shown in the measurements.

Table 5: Wave Frequency Surge and Sway % Damping

	1	2	3	4	5	6	7	8	9	Ave.
Surge	12.3	13.2	11.5	11.6	11.3	9.9	10.7	13.3	9.4	11.5
Sway	11.4	11.4	12.7	11.3	11.9	10.7	13.5	15.1	9.0	11.9

Table 6: Resonance Roll and Pitch % Damping

	1	2	3	4	5	6	7	8	9	Ave.
Roll	2.68	2.68	2.52	2.85	2.85	3.33	2.85	3.17	2.19	2.79
Pitch	2.85	2.35	2.52	2.52	3.01	2.52	2.19	2.52	2.52	2.56

4.3 Response Comparisons: Theory vs. Measurement

A peak hurricane sea state was assumed based on the hindcast¹ wave data, with significant wave height $H_s = 36.85$ ft and spectral peak period $T_p = 13.0$ sec for use in a JONSWAP spectrum with a peak shape factor equal to 3.3. This was the maximum sea state according to the hindcast and occurred during the second three-hour time interval. A theoretical response spectrum was then obtained using the transfer functions derived from numerical models of Brutus. The theoretical power spectrum of response was then compared with the results from a spectral analysis of the measured data. The measured spectrums for the first, second, and third time intervals, corresponding to the three hours prior, during, and after the hurricane peak are included for comparison.

The transfer functions were for tendon top tension for head, beam, and quartering sea conditions, without current and wind effects. The measured response spectrums contain wind and current energy for a continually transient sea state, contributing to possible differences in response. The spectral limitations of the model and full-scale measurements must also be recognized. The numerical model transfer functions only yield response results between .04 and .3 Hz, with a frequency step of .004 Hz, which is coarse in comparison to the measured tendon responses, with a range of 0 to 1 Hz and frequency steps of $6.0E^{-4}$ Hz.

The measured response spectrums have their typical spectral limitations as well, mainly non-stationarity and “jaggedness” as discussed in 4.2. For simplicity, the measured tendon tension PSDs used in the comparison were generated using three hours of data, whereas all other frequency domain

calculations used the hourly data. The tendon response spectrum comparisons can be seen in Figures 5 to 8.

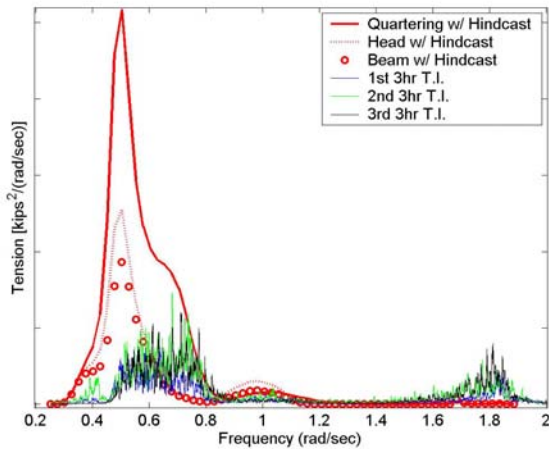


Figure 5: T2 Response Comparison

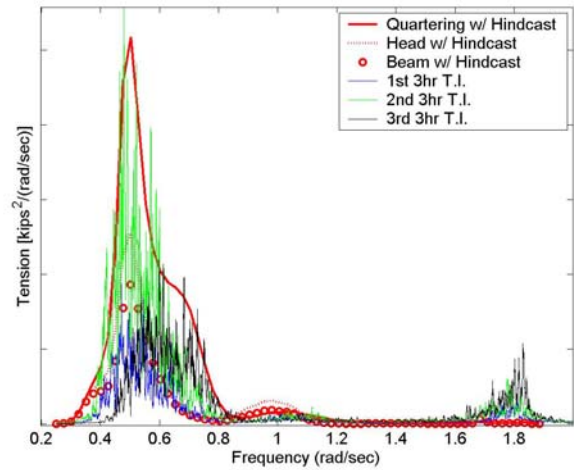


Figure 8: T11 Response Comparison

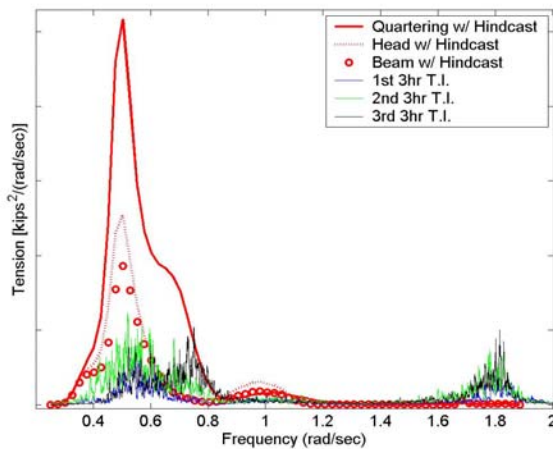


Figure 6: T5 Response Comparison

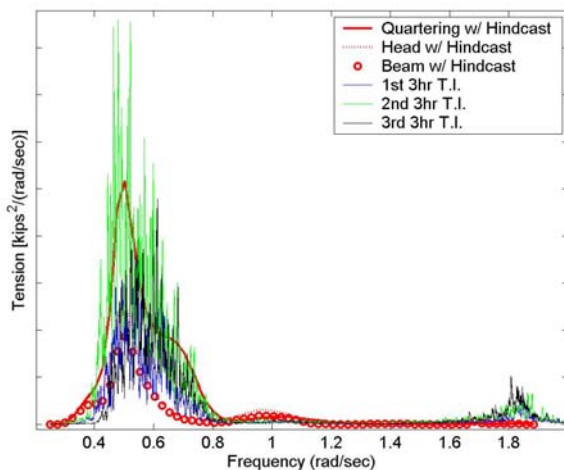


Figure 7: T8 Response Comparison

The comparison between tendon response spectrums shows the tendons behaving in pairs. The magnitude and shape of the wave energy response for the tendon pairs, T2 & T5, and T8 & T11, differ substantially. The measured responses for tendon pair T2 & T5, shown in Figures 5 and 6, exhibit much lower magnitudes than the theoretical responses for all directions. However, the theoretical responses for tendon pair T8 & T11, shown in Figures 7 and 8, exhibit magnitudes on par with those obtained from the measurements. It is also important to notice that the measured spectrums for tendons T2 & T5 do not exhibit the same energy peak, at .5 rad/sec, as tendons T8 & T11 and predicted by theory. Tendons T8 and T11 had larger maximums and greater variability than the other two tendons, which is consistent with increased energy content.

Directionality of the environment is one possible explanation for the difference in energy content between tendon pairs, however the measured spectrums for T2 & T5 fail to match those predicted for any direction. The wave directions provided by the hindcast for these nine hours range from 260° to 330°. Waves traveling in these directions for Brutus are best described by quartering seas. Comparisons between the quartering sea spectrums and those for T8 & T11 for the second time interval match the best. The first and third time intervals for T8 & T11 do not match as well to the quartering sea model simply because the seas were building and dropping during these periods.

In general, the comparisons indicate that environment direction may significantly contribute to tendon response. Although the tendon transfer functions do not accurately represent the individual tendon energy for a particular direction, the maximum energy is well captured for a design basis.

5 TIME DOMAIN RESULTS

5.1 Statistical Analysis of Tendon Tensions

The time domain analysis provides performance statistics such as means, maximums, minimums and standard deviations. For the time domain analysis the hurricane was broken down into three consecutive three-hour long time series. Three-hour sea states were chosen to match those typically used in physical model tests and computational models. Statistics for each tendon and sea state were then computed thus providing a direct comparison to design predictions.

The tendon tensions statistics for the entire time series, normalized by the appropriate design value are given in Table 7. Likewise, the results for the various 3-hour periods are given in Table 8. The mean measured tensions were normalized by the pre-tension. The measured mean tensions exceeded the pre-tension by 6 – 9% probably due to water level variations. All maximum measured responses are well below (20–25% lower) the corresponding design values. The minimum tendon tension was normalized by the design maximum tendon tension and it can be seen that the tendons were nowhere near a critical condition of a loss of tendon tension.

Table 7: Tendon Tensions for Entire Time Series

(Normalized by Design Values)

	T2	T5	T8	T11
Maximum	0.75	0.71	0.81	0.76
Minimum	0.38	0.36	0.25	0.28
Mean	1.09	1.07	1.06	1.06
Coefficient of Variation	0.09	0.10	0.10	0.08

Table 8 shows how the statistics changed during the passing of the hurricane, which is an indication of the non-stationary nature of the hurricane process.

Table 8: Tendon Tension for each Sea State

(Normalized by Design Values)

Hours	1-3	3-6	6-9	9-12	12-15	15-18	18-21
T2 mean	1.03	1.03	1.02	1.06	1.23	1.17	1.09
T5 mean	1.01	1.01	0.98	1.00	1.12	1.20	1.17
T8 mean	1.01	1.01	1.00	1.03	1.11	1.13	1.10
T11 mean	1.02	1.02	1.01	1.05	1.12	1.10	1.08
T2 CoV	0.03	0.04	0.04	0.06	0.09	0.08	0.05
T5 CoV	0.02	0.03	0.03	0.05	0.10	0.07	0.05
T8 CoV	0.03	0.06	0.06	0.10	0.14	0.11	0.06
T11 CoV	0.02	0.04	0.04	0.07	0.11	0.09	0.06

5.2 Probability Distribution of Tendon Tensions

A comparison between measured peak tendon tensions and the values implied by a Rayleigh distribution (straight line in the plots) may be viewed in Figures 9 to 12. Each tendon has at least one maximum and minimum peak that deviates from the Rayleigh distribution but the deviations are consistent with those usually observed from model tests and included in design.

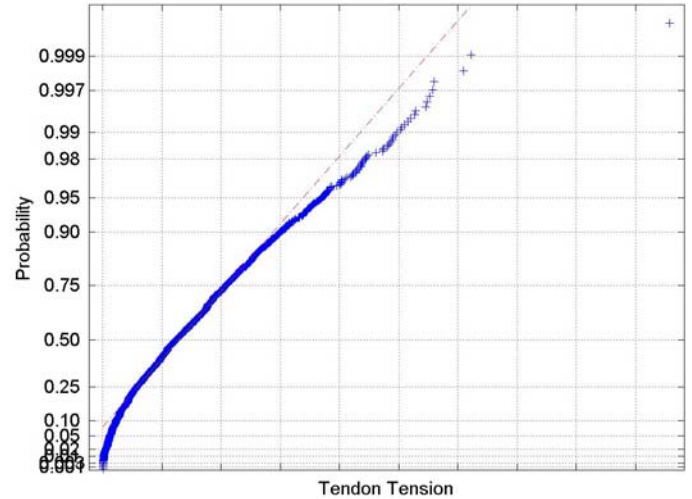


Figure 9: Probability of T2 Peak Tension for First 3hrs

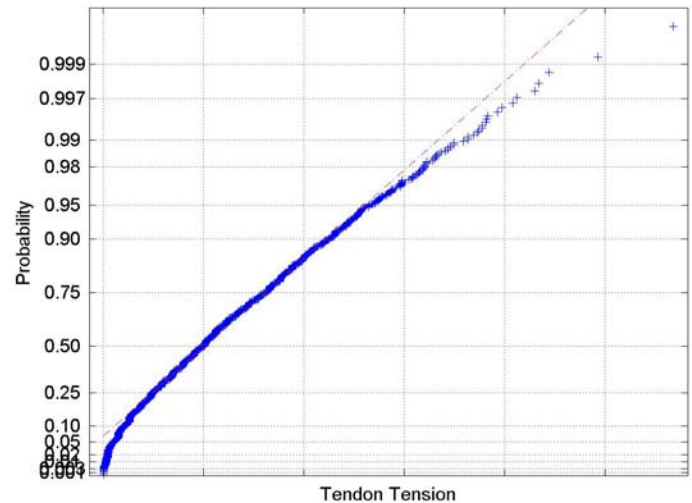


Figure 10: Probability of T5 Peak Tension for First 3hrs

Table 9: Measured Γ Values

Hours	Max Tension				Min Tension			
	3	6	9	Ave	3	6	9	Ave
T2	5.0	3.2	4.3	4.2	5.6	5.0	5.9	5.5
T5	2.6	3.1	2.9	2.9	7.2	4.7	5.8	5.9
T8	3.3	3.8	4.7	3.9	5.9	5.0	6.4	5.7
T11	2.4	3.9	5.2	3.8	7.0	6.1	6.5	6.5

6. VORTEX SHEDDING EFFECTS

Although traditional spectral techniques are informative they give little indication of the energy evolution with respect to time, which is important for a non-stationary process like a hurricane. The spectrogram provides spectral energy with respect to time and, as time and frequency resolutions are inversely related, an informative balance is conveyed to the reader. Spectrograms are explained in more detail in the open literature³⁴. Frequency and time are plotted along the axes, while energy intensity is represented by color, with red and blue being the maximum and minimum energy, respectively.

Figure 13 gives the spectrogram for T2 tendon tensions for the entire twenty-one hour time series. Not only can the natural frequencies and wave energy be identified in the spectrogram as with a PSD, but the evolution of the energy may be seen. The wave energy, approximately .1 Hz, is a prime example of time dependency. At the beginning of the time series, the wave energy is predominately yellow. As the hurricane impacts Brutus, at approximately 4×10^4 seconds, the wave energy increases and becomes predominately red.

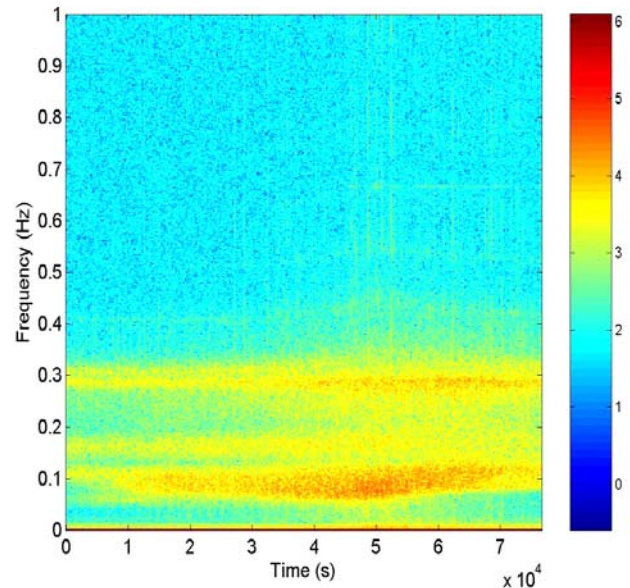


Figure 13 – Spectrogram for T2

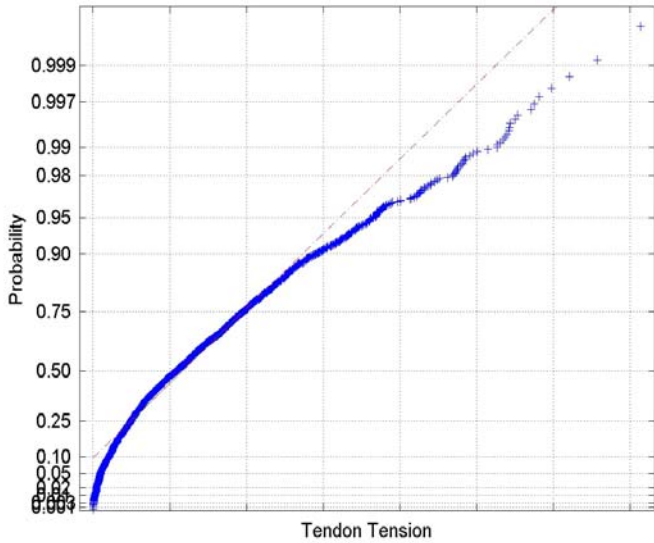


Figure 11: Probability of T8 Peak Tension for Second 3hrs

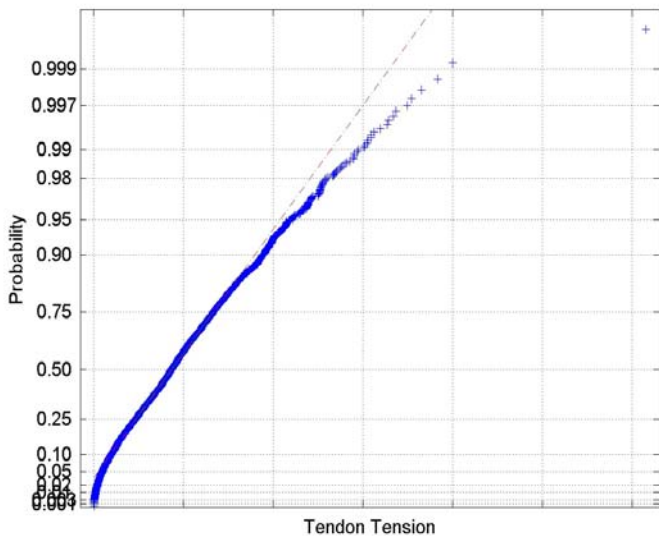


Figure 12: Probability of T11 Peak Tension for Third 3hrs

The calculated Γ values (equations 3 and 4) for maximum and minimum tensions may be seen in Table 9. The measured Γ values for maximum and minimum tendon tensions exhibit great variability, which is consistent with the results of model tests²⁹.

Γ values vary for each tendon and sea state. Minimum tension Γ values are much larger than maximum tension Γ values suggesting that minimum tendon tensions were more non-linear than maximum tendon tensions.

Vortex shedding excitation of risers, flow lines and tendons is a vital concern for every floating platform. The spectrogram allows for such modes to be easily identified. The spectrogram for T2, Figure 13, shows a faint yellow band of energy at around 0.45 Hz representing the first vortex shedding mode. As time progresses and the hurricane intensity increases, the vortex shedding modal frequency also increases. The change in modal frequency is analogous to tightening a guitar string. Increasing or decreasing tension produces parallel changes in modal frequencies. For Brutus, the mean tendon tension is increasing because of the increased platform offset during the peak of the hurricane. Higher vortex shedding modes exhibit the same characteristic and may be viewed (albeit faint) as well.

Due to resolution issues and differences in relative wave and vortex shedding energy, the spectrogram permits the identification of the presence of vortex shedding modes but is less certain in terms of quantifying the magnitude of such effects. The spectrogram may provide more useful information during loop current events²⁸ where differences between wave and vortex shedding energy are less pronounced. Increasing the sampling frequency would also provide more vortex shedding modal information.

The magnitude of the vortex shedding effects can be roughly estimated from the tendon tension PSD in Figure 14. The vortex shedding excitation spikes are clear for the frequency range exceeding 3 rad/sec. By integrating the energy in this frequency bands a significant tendon tension value of around 25 kips was estimated. Such additional tension was not of concern as shown by the maximum and minimum tendon tensions discussed in the time-domain results.

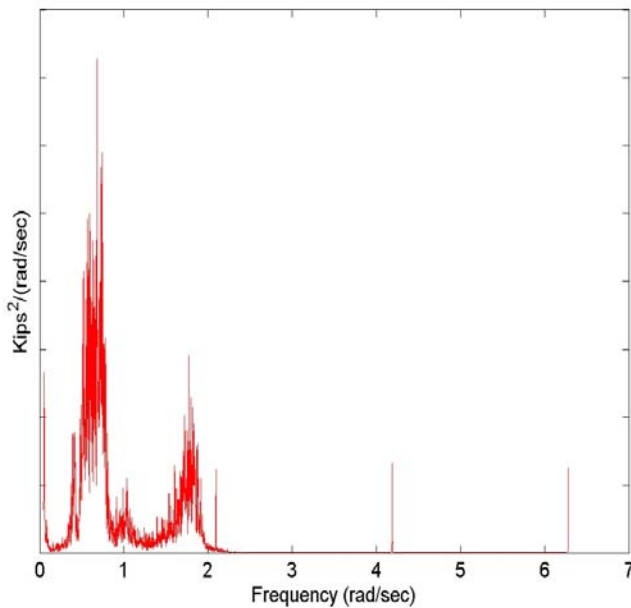


Figure 14 – PSD for T2 Tendon Tension

7. CONCLUSIONS AND RECOMMENDATIONS

- Although the peak environmental conditions during Lili approached 100-year values, the measured responses for Brutus were well below the design limits.
- The most likely explanation for this favorable outcome is that Lili's behavior was fundamentally different from the following standard design assumptions:
 - Peak environmental conditions lasting for 3-hours
 - Constant direction of environmental loading
 - Stationary narrow-banded process
 - Collinear wave, wind and current
- Comparisons between measured and predicted tendon response spectrums emphasized the importance of environment directionality on response.
- The apparent lack of response of some of the tendons in Brutus at the wave frequency range was intriguing and a departure from numerical models.
- The damping estimated from the measurements was reasonably consistent with the values used in design but it is noted that the roll and pitch resonance in the measurements may contain heave resonance as well, since their respective natural frequencies are nearly identical and difficult to filter out. This feature could have an influence in the larger damping estimates given by the measurements.
- Design practices for TLPs usually predict maximum tendon tension by combining components due to pretension at mean sea level, tide / surge variation, overturning due to wind and current, set down due to static and slowly varying offset, wave forces and wave induced motion about the mean offset, foundation mispositioning, ringing / springing, tendon load sharing, vortex shedding and general design margins. A conservative combination is developed relative to a representative environmental event such as Lili.
- Minimum tendon tension is an important criterion for TLPs and it was noted that the minimum tendon tensions during Lili did not approach zero at all for Brutus. This is also a positive indication of the performance of TLPs under a major event such as Hurricane Lili.
- Some tendon tensions indicated a clearly non-Gaussian quality to their response due to non-linearity in either the environmental conditions or the TLP response itself (or both). The non-Gaussian nature of tendon tension response is usually captured in design by empirical factors based on model testing and numerical models. TLP designers should maintain care and diligence in performing and interpreting model tests and validating their numerical models.
- Feasible theoretical improvements to capture such non-Gaussian response with perhaps less reliance on empirical model test data include the use of Generalized Extreme Value distributions³⁵ as well as application¹³ of a Hermite Polynomial model. Another potentially helpful advance³⁶ is the application of a multivariate statistical description to the sea climate, in order to estimate extreme response.

- Vortex shedding excitation of the tendons was observed but its contribution to the total tendon tension was not of concern.
- The monitoring data for the TLPs indicated the robustness of current global performance analysis methods but further investigation is necessary to indicate how such design methods could be improved. As noted, loss of tendon tension is an important criterion in TLP design but tendon tensions during Lili remained relatively high – this is an area where further investigation may lead to more economical designs.
- Extensive literature is available related to reliability based methods for TLP design. A co-coordinated effort is proposed to collate such information and develop a risk-based approach to the design and operation of TLPs worldwide.

ACKNOWLEDGMENTS

The authors gratefully acknowledge Shell International E & P, Inc. for providing the monitoring data for this study and the US Minerals Management Service for funding this study. Peter Young and George Rodenbusch of Shell International E & P, Inc. provided overall support and useful discussions on the work. Any opinion, findings, and conclusions or recommendations expressed in this paper are those of the authors.

REFERENCES

- [1] Cardone, V.J., Cox, A.T., Lisaeter, K.A., Szabo, D., 2004, "Hindcast of winds, waves and currents in Northern Gulf of Mexico in Hurricane Lili (2002)". Proc. of Offshore Technology Conference, Houston, Texas.
- [2] Morandi, A.C., Mercier, J.A., Bea, R.G., 2004, "Performance of deepwater floating production facilities during Hurricane Lili," Proc. of Offshore Technology Conference, Houston, Texas.
- [3] Leverette, S.J., Rashedi, R., 1995, "Reliability-based design methodology for TLP design," Proc. of 4th SNAME Offshore Symposium, Houston, Texas.
- [4] Mercier, J.A., 1991, "Reliability-based design code for floating systems," Proc. of 2nd SNAME Offshore Symposium, Houston, Texas.
- [5] Banon, H., Toro, G., Jeffreys, R., 1994, "Development of reliability-based global design equations for TLPs," Proc. of the 13th International Conference on Offshore Mechanics and Arctic Engineering, OMAE'94, Houston, Texas.
- [6] Mathisen, J., Rashedi, R., Moerk, K., Zimmer, R., Skjong, R., 1994, "Reliability-based load and resistance factor design code for TLP hull structure," Proc. of the 13th International Conference on Offshore Mechanics and Arctic Engineering, OMAE'94, Houston, Texas.
- [7] Leverette, Bradley and Bliault, 1982, "An integrated approach to setting environmental design criteria for floating production facilities," Proc. of Behavior of Offshore Structures, BOSS'82.
- [8] Bea, R.G., Allin Cornell, C., Vinnem, J.E., Geyer, J.F., Shoup, G.J., Stahl, B., 1992, "Comparative risk assessment of alternative TLP systems: Structure and foundation aspects," Proc. of the 11th International Conference on Offshore Mechanics and Arctic Engineering, OMAE'92, Calgary, Canada.
- [9] Kung, C.J., Wirsching, P.H., 1992, "Fatigue and fracture reliability and maintainability of TLP tendons," Proc. of the 11th International Conference on Offshore Mechanics and Arctic Engineering, OMAE'92, Calgary, Canada.
- [10] Hovde, G., Moan, T., 1994, "Fatigue reliability of TLP tether systems," Proc. of the 13th International Conference on Offshore Mechanics and Arctic Engineering, OMAE'94, Houston, Texas.
- [11] Ang, A. H.-S., 1986, "A study of the reliability of a Tension Leg Platform," Report No. CG-M-1-86, 2, US Coast Guard Office of Marine Safety, Security and Environmental Protection, Washington, D.C.
- [12] Naess, A., Ness, G.M., 1992, "Second-order, sum-frequency response statistics of tethered platforms in random waves," Applied Ocean Research, 14, No.1, pp. 23-32.
- [13] Winterstein, S., Marthinsen, T., 1991, "Nonlinear effects on TLP springing response and reliability," Proc. 1st Intl. Conf. Computational Stochastic Mechanics. Ed. P.D. Spanos and C.A. Brebbia, Computational Mechanics Publications, Southampton.
- [14] Naess, A., Moe, G., 1992, "The statistics of springing response of a TLP," Proc. of the 11th International Conference on Offshore Mechanics and Arctic Engineering, OMAE'92, Calgary, Canada.
- [15] Banon, H., Harding, S.J., 1989, "Methodology for assessing reliability of Tension Leg Platform tethers," Journal of Structural Engineering, 115, No. 9, pp. 335-344, Houston.
- [16] Das, P.K., Faulkner, D., Guedes da Silva, A., 1991, "Limit state formulations and modeling for reliability-based analyses of orthogonally stiffened cylindrical shell structural components," Rep. NAOE-91-26, Dept. Naval Architecture and Ocean Engineering, Glasgow University.
- [17] Faulkner, D., Birrel, N.D., Stiansen, S.G., 1983, "Development of a reliability-based code for the structure of tension leg platforms," Proc. of Offshore Technology Conference, Houston.
- [18] Lotsberg, I., 1991, "Probabilistic design of the tethers of a Tension Leg Platform," J. Offshore Mechanics and Arctic Engineering, 113, pp. 162-170.
- [19] Rooney, P., Lereim, J., Madsen, H.O., 1989, "Application of probabilistic methods for verification and

- calibration of a TLP tether system design based on partial coefficients,” Proc. of the 8th International Conference on Offshore Mechanics and Arctic Engineering, OMAE’89, The Hague, Netherlands.
- [20] Stahl, B., Geyer, J.F., 1985, “Ultimate strength reliability of Tension Leg Platform systems,” Proc. of Offshore Technology Conference, Houston, Texas.
- [21] Ximenes, M.C.C., Mansour, A.E., 1991, “Fatigue system reliability of TLP tendons including inspection updating,” Proc. of the 10th International Conference on Offshore Mechanics and Arctic Engineering, OMAE’91.
- [22] Stansberg, C.T., “Statistical properties of nonlinear wave-induced high frequency responses in random waves,” Proc. Seminar on Tensioned Buoyant Platforms, University College London, Bentham Press, London.
- [23] Mercier, J.A., Leverette, S.J., Bilault, A.L., 1982, “Evaluation of Hutton TLP response to environmental loads,” Proc. of Offshore Technology Conference, Houston, Texas.
- [24] Erb, P.R., Finch, C.L., Manley, G.R., 1985, “The Hutton TLP Performance Monitoring and Verification Program,” Proc. of Offshore Technology Conference, OTC 4951, Houston, Texas.
- [25] Hauch, S. and Haver, S., 1998, “Measured Motion Characteristics of the Heidrun TLP,” Proc. of the 17th International Conference on Offshore Mechanics and Arctic Engineering, OMAE98-1391.
- [26] Marthinsen, T., Muren, J., 1993, “Snorre TLP – comparison of predicted and measured response, Proc. Seminar on Tensioned Buoyant Platforms,” University College London, Bentham Press, London.
- [27] American Petroleum Institute, 1997, “Recommended practice for planning, designing and constructing tension leg platforms,” 2nd Ed., Washington, DC.
- [28] Leverette, S., Rijken, O., Dooley, W., Thompson, H., 2003, “Analysis of TLP VIV responses to Eddy Currents,” Proc. of Offshore Technology Conference, Houston, Texas.
- [29] Young, P., 1998, “Brutus TLP Global Performance Verification,” Shell International Exploration and Production Inc. Houston, Texas.
- [30] Campbell, R.B. and Vandiver, J.K., 1980, “The Estimation of Natural Frequencies and Damping Ratios of Offshore Structures,” Proc. of Offshore Technology Conference, OTC 3861, Houston, Texas.
- [31] Garrett, D.L., Gu, G.Z., Watters, A.J., 1995, “Frequency Content Selection for Dynamic Analysis of Marine Systems,” Proc. of the 14th International Conference on Offshore Mechanics and Arctic Engineering, OMAE’95, 1, pp 393-399.
- [32] Kijewski, T. and Kareem, A., 1999, “Analysis of Full-Scale Data from a tall building in Boston: Damping Estimates,” Proc. of the 10th International Conference on Wind Engineering.
- [33] Kurtis, G. and Kareem, A., 1999, “Applications of Wavelet Transforms in Earthquake, Wind and Ocean Engineering, Engineering Structures,” 21, pp. 149-167.
- [34] Oppenheim, A.V. and R.W., Schafer, 1989, “Discrete-Time Signal Processing,” Prentice-Hall, pp. 713-718.
- [35] Voortman, H.G., Van Gelder, P.H.A.J.M., and Vrijling, J.K., 1999. “Reliability analysis of the dynamic behavior of vertical breakwaters”, In: Safety and Reliability, Vol. 1, pp.519-524, downloadable from: <http://www.hydraulicengineering.tudelft.nl/public/gelder/aper32.pdf>.
- [36] Repko, A., Van Gelder, P.H.A.J.M., Voortman, H.G. Vrijling, J.K., “Bivariate statistical analysis of wave climates”, Proceedings of the 27th ICCE, Vol. 1, pp. 583-596, Coastal Engineering 2000, Sydney, Australia, 16-21 July 2000, Ed. Billy L. Edge, ASCE.